JGR Oceans

RESEARCH ARTICLE
10.1029/2023JC020055

Spatial and Interannual Variability of Antarctic Sea Ice Bottom Algal Habitat, 2004–2019

Stephanie M. Lim[1], Gert L. van Dijken[1], and Kevin R. Arrigo[1]

[1]Department of Earth System Science, Stanford University, Stanford, CA, USA

Key Points:

- About 81% of Antarctic sea ice cover transmitted sufficient light to the bottom ice to support ≥2 weeks of net ice algal growth each year
- An increase in the proportion of habitable area prevented a decline in potential habitat during the 2016–2019 reduction in sea ice area
- Potential habitat was highly spatially variable and best explained by bottom ice melt date. It is likely sensitive to future climate change

Supporting Information:

Supporting Information may be found in the online version of this article.

Correspondence to:

S. M. Lim,
smlim@stanford.edu

Citation:

Lim, S. M., van Dijken, G. L., & Arrigo, K. R. (2023). Spatial and interannual variability of Antarctic sea ice bottom algal habitat, 2004–2019. *Journal of Geophysical Research: Oceans*, *128*, e2023JC020055. https://doi.org/10.1029/2023JC020055

Received 19 MAY 2023
Accepted 7 SEP 2023

Abstract In the Antarctic, sea ice algae use the highly dynamic sea ice as a platform for growth. Antarctic sea ice extent has recently been highly variable, first showing a slight increase and then a record decrease starting in 2016. We investigated the response of Antarctic ice algal habitat to variations in sea ice and other environmental forcings during 2004–2019. Combining an ice growth model, remote sensing and reanalysis data, and a radiative transfer model, we assessed whether light penetration to the bottom ice was sufficient for ice algal growth. Trends in the inputs over the 16 years were relatively small: there were no changes in ice thickness or bottom ice melt date, a 6.4% decrease in snow depth, a 1.2% decrease in incident light, and a 0.8°C decrease in air temperatures. Eighty-one percent of the sea ice cover was habitable by ice algae for ≥14 days each year. The Antarctic has a larger extent and duration of potential ice algal habitat than the Arctic. Over time, the spatially averaged seasonal duration of habitat increased because a higher proportion of each pixel became habitable on average, compensating for the 2016–2019 reduction in sea ice extent. The spatial variability in potential habitat was strikingly high, even within geographic sectors. Bottom ice melt date (bloom termination) far surpassed other environmental factors in explaining variation (45%) in ice algal habitat on the 25 km scale. Because melt date depends on the ice-atmosphere heat balance, Antarctic ice algal habitat may be highly sensitive to future climate changes.

Plain Language Summary Sea ice algae are single-celled photosynthetic organisms that grow within or at the bottom of sea ice. They tend to bloom early in the spring each year before other carbon fixers and are therefore an important food source for small marine animals. We examined how ice algae responded to spatial and temporal changes in the Antarctic environment during 2004–2019, a period that featured large swings in the amount of area covered by sea ice. We paired satellite data, which can measure where sea ice is and the depth of the snow on top of the ice, with other atmospheric data (e.g., incoming sunlight and air temperature) from models and observations to estimate where and when sea ice was potential algal habitat. There were some increases in habitable sea ice, but more importantly, we found that the spatial distribution of habitat was very patchy. This spatial unevenness suggests that whether or not sea ice is habitable is highly affected by relatively small changes in the environment and that ice algae may be quite sensitive to future climate changes.

1. Introduction

Relying on sea ice as a platform for growth, Antarctic ice algae are adapted to one of the most dynamic and extreme ecosystems on Earth. Living within or at the bottom of sea ice, ice algae often contend with confined, cold, and highly saline growing spaces. Depending on the history and conditions of the sea ice, algae can grow within the bottom ice, in strands attached to the bottom ice, in internal brine pockets and channels, and near the snow-ice surface, often after surface flooding caused by a heavy snow cover (a "slush" layer; Arrigo, 2017). Ice algae must make use of extremely low light levels as the Antarctic emerges from polar night and because the overlying snow and sea ice are strong attenuators of light. The sea ice itself is strikingly seasonal, as the Antarctic retains only a small fraction of its sea ice through the summer: 2–3 million km^2 largely concentrated in the Weddell Sea and secondarily in the Bellingshausen and Amundsen Seas (Fetterer et al., 2017). 15–17 million km^2 of new ice is formed each year.

The response of Antarctic sea ice to climate patterns during the satellite era has been inconsistent. For one, the Antarctic is affected by strong climate oscillations including the Southern Annular Mode (SAM) and the Southern Oscillation, which result in high interannual variability in the sea ice environment and challenge our ability to distinguish long-term climate trends (Eayrs et al., 2021). Using sea ice extent as an example, during

1979–2014, annual mean ice extent increased at a rate of 0.0224 million km^2 year^{-1}, reaching a record high in 2014 (Parkinson, 2019). However, 2016 marked the beginning of a precipitous reduction in sea ice, with a 2.1 million km^2 decrease in annual mean extent over three years—the equivalent of 30 years of sea ice loss in the Arctic (Eayrs et al., 2021; Parkinson, 2019). Although sea ice extent appeared to recover to climatological levels by summer 2020, the Antarctic sea ice extent reached a record low in summer 2022 (1.9 million km^2; Raphael & Handcock, 2022; Wang et al., 2022) and prompted suggestions that the Antarctic is falling into a new regime or state (Raphael & Handcock, 2022).

These recent and severe fluctuations in the sea ice environment emphasize the importance of estimating the current state of Antarctic ice algae and their response to recent swings in sea ice conditions. Ice algae are estimated to contribute only 1% of annual primary production in the Southern Ocean south of 50°S, but contribute a higher proportion of production in the early season (4% in November) and in the sea ice zone (2%–24% annually; reviewed in Arrigo, 2017). As a result of both the timing and location of ice algal blooms, they serve as an important food source for zooplankton and ice-associated grazers. Short-term fatty acid analyses found that an average of 40%–60% of carbon in seven species of Antarctic zooplankton in August–October had ice algal origins (Kohlbach et al., 2018). The "keystone" species of Antarctic krill similarly features up to 56% and 88% ice algal-derived carbon in adults and juveniles, respectively (Kohlbach et al., 2017). Fatty acids that integrate over a longer period show less reliance on ice algae as the season progresses (Kohlbach et al., 2018, 2017), as most grazers have plastic feeding styles that can switch to pelagic food sources. Similar seasonal patterns are seen in markers in Antarctic seabirds and seals (Goutte et al., 2014). Overall, ice algae are a key overwintering and spring food source for zooplankton before ice retreat and phytoplankton blooms. They may also serve to seed phytoplankton blooms, supply polyunsaturated fatty acids and ultraviolet radiation-absorbing compounds to other marine organisms, and/or contribute to the carbon flux to the benthos (reviewed in Arrigo & Thomas, 2004).

To investigate the potential distributions of these important primary producers in the ice-covered Southern Ocean, we quantified the extent and duration of Antarctic ice algal habitat over the 2004–2019 period. Using remote sensing and reanalysis data, an idealized thermodynamic ice growth model, and a radiative transfer model, we defined sea ice as being habitable when enough light is transmitted to the bottom ice in a given day to support algal growth in spring. Although the interior and upper sea ice (e.g., slush layers) can also serve as habitat for ice algae, we focused on the bottom ice where ∼80% of primary production is concentrated (Saenz & Arrigo, 2014) and where it is easier to constrain habitable conditions. We related the interannual and the large- and small-scale spatial variability in potential habitat to environmental variables in order to illuminate the major controls on the extent and duration of Antarctic ice algal habitat.

2. Methods

1Antarctic ice algal habitat was determined in a method similar to Lim et al. (2022). Briefly, light transmission to the bottom ice algal layer (0.05 m, Table 1) was calculated using two spectral radiative transfer models: a cloud-corrected atmospheric model (Arrigo et al., 1998; Dobson & Smith, 1988; Gregg & Carder, 1990) and one through the snow and ice layers (Arrigo et al., 1991). Light absorption by ice algae in the surface and internal ice was neglected. For each location, net chlorophyll-*a* (Chl*a*)-specific photosynthetic rates for ice algae were calculated every 3 hr based on the transmitted photosynthetically active radiation (PAR; 400–700 nm) and then integrated over the course of 1 day. If this net photosynthetic rate (corrected for respiration) was >0 g C g^{-1} Chl*a* for the day, then the ice was considered potential habitat for ice algae, unless ice at that grid cell had already started melting that year.

2.1. Sea Ice Thickness Model

A key modification of the method described in Lim et al. (2022) involves the determination of ice thickness (Figure 1a). In Lim et al. (2022), sea ice thickness was estimated from ice age, taking advantage of the long satellite record of ice age in the Arctic Ocean. Given the absence of an equivalent ice age data set for the Antarctic—which again has mostly first-year ice (Fetterer et al., 2017)—vertical sea ice growth was estimated thermodynamically by balancing the heat flux out of the ice to the ocean and atmosphere with the heat released by freezing ice and accounting for sea ice motion. Our model produces sea ice thickness at the same scale, 25 km, obtained by passive microwave observations of sea ice, relying on a combination of forcing data sets

Table 1
Ice Growth Model and Algal Habitat Assessment Parameters

Parameter	Standard run value	Units	Reference
ρ_i	920,000	g m^{-3}	Behrendt et al. (2015)
F_w	5.02	W m^{-2}	Arrigo et al. (1993)
L_i	334	J g^{-1}	Behrendt et al. (2015)
λ_i	2.2	W m^{-1} K^{-1}	Lei et al. (2010)
λ_s	0.2	W m^{-1} K^{-1}	Behrendt et al. (2015) and Pringle et al. (2007)
k	60	W m^{-2} K^{-1}	Behrendt et al. (2015)
$P^*_{\max}$	0.64	g C g^{-1} Chl$a$ h^{-1}	See Section 2.2
α^*	0.062	g C g^{-1} Chl$a$ h^{-1} [μmol photons m^{-2} s^{-1}]$^{-1}$	See Section 2.2
R^*	0.083	g C g^{-1} Chl$a$ h^{-1}	See Section 2.2
Scattering layer thickness	0.30	m	Perovich (2002)
K_d dry snow	22.33[a]	m^{-1}	Perovich et al. (1986)
K_d scattering ice	5.35[a]	m^{-1}	Perovich et al. (1986)
K_d interior ice	1.68[a]	m^{-1}	Perovich et al. (1986)
Algal layer location	0.05[b]	m	van Leeuwe et al. (2018)

[a]Diffuse attenuation coefficients (K_d) are spectral; here we report the mean for 400–700 nm. [b]Measured from the ice-water interface at the bottom of the sea ice.

(Section 2.3) and processes at different temporal and spatial scales: daily snow depth (Figure 1b), 2 m air temperatures every 6 hr (Figure 1c), daily sea ice concentrations, and daily sea ice motion. Due to this combination of processes, we consider the ice growth model somewhat specialized for estimating Antarctic sea ice thickness at the 25 km scale and for the ensuing ice algal habitat assessment. Other estimates, such as satellite altimetry, earth system models, or data-assimilating models, may be better suited for different research questions regarding Antarctic sea ice.

2.1.1. Thermodynamic Ice Growth and Ice Motion

We calculated daily sea ice thickness from thermodynamic growth and ice motion. The net conductive heat flux out of the ice was assumed to be fully balanced by the release of latent heat, L_i (J g^{-1}), during freezing (Petrich & Eicken, 2017):

$$\rho_i L_i \frac{dH}{dt} = F_c - F_w. \quad (1)$$

The left side of the equation represents sea ice growth via freezing, where ρ_i is the bulk density of the ice (g m^{-3}), H is the ice thickness (m), t is time (s), and the right side of the equation represents the difference in the conductive heat fluxes (W m^{-2}) between the ice and the atmosphere, F_c, and between the ice and the ocean, F_w.

Because Antarctic sea ice usually has a layer of snow, we treated the ice as two layers (Behrendt et al., 2015; Petrich & Eicken, 2017):

$$F_c = \frac{T_w - T_0}{\frac{H}{\lambda_i} + \frac{h}{\lambda_s}} \quad (2)$$

where T_w is the water temperature set to a constant 271.35 K (−1.8°C), T_0 is the surface snow temperature, h is the snow depth (m), λ_i is the thermal conductivity of ice (W m^{-1} K^{-1}), and λ_s is the thermal conductivity of snow (W m^{-1} K^{-1}).

The heat flux between the snow surface and the atmosphere, F_a (W m^{-2}), was linearly approximated as $F_a = k(T_0 - T_a)$ (Leppäranta, 1993) in order to use the 2 m air temperature T_a, instead of T_0, which is unknown. k is an effective heat transfer coefficient that approximates both turbulent and net longwave radiative fluxes (W m^{-2} K^{-1}). Its value depends on various atmospheric conditions (wind speed, snow insulation, radiation,

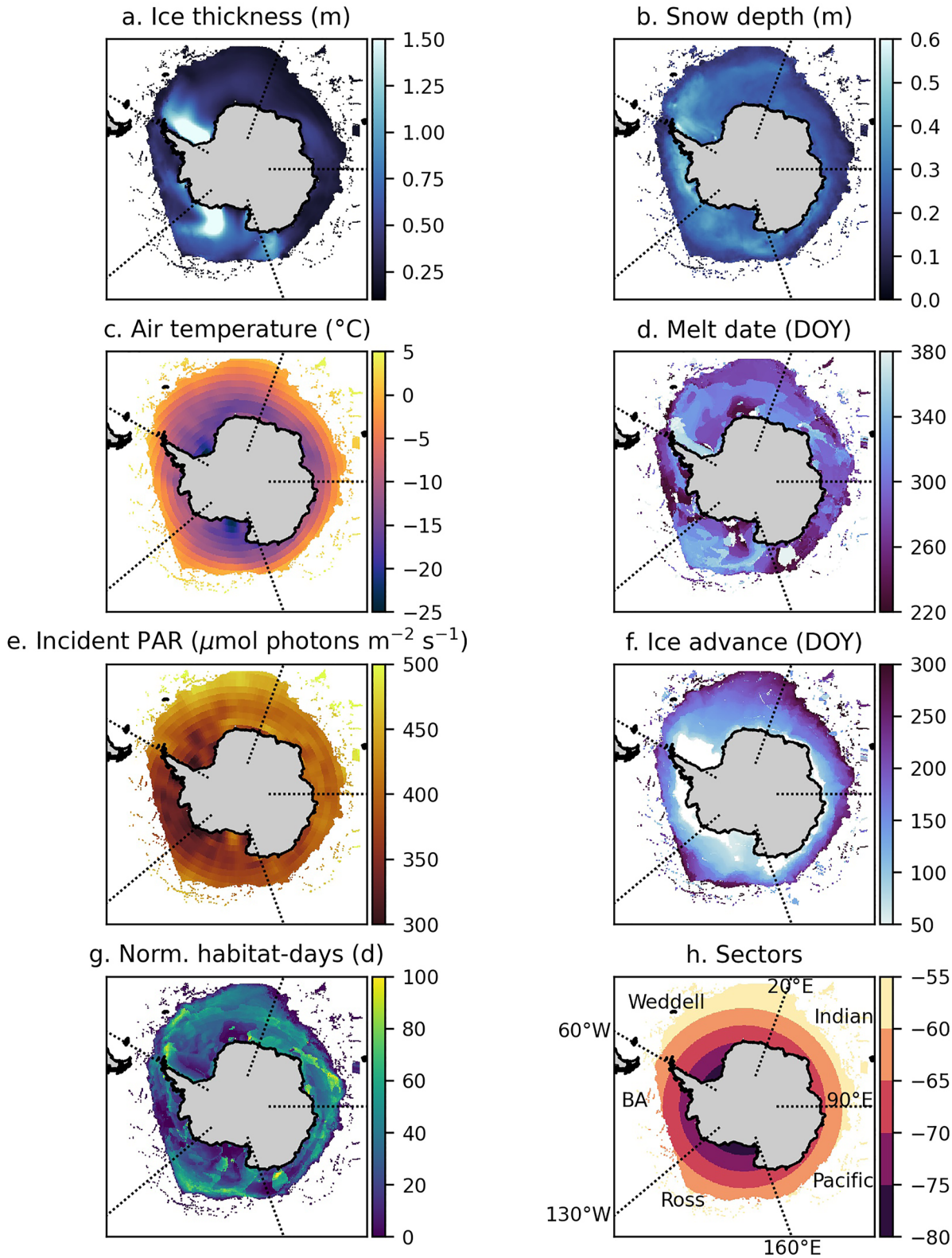

Figure 1. Examples of ice algal habitat assessment inputs and outputs for a typical year (2005): (a) sea ice thickness, (b) snow depth, (c) air temperature, (d) melt date as day of the year (DOY) in 2005, which can be greater than 365 because melt is allowed through 31 January 2006, (e) downwelling incident photosynthetically active radiation (PAR), (f) date of ice advance, and (g) ice algal normalized habitat-days. (a–c) and (e) are averaged June–January, while (d, f, and g) are annual metrics. (h) shows latitude and labels the sectors used in this analysis, where BA is Bellingshausen-Amundsen.

humidity, evaporation, and atmospheric stability) but here we use a constant (Table 1). Then assuming that $F_a = F_c$ (Leppäranta, 1993), Equation 2 becomes:

$$F_c = \frac{T_w - T_a}{\frac{1}{k} + \frac{H}{\lambda_i} + \frac{h}{\lambda_s}}. \tag{3}$$

Combining Equations 1 and 3 and solving for the rate of change of sea ice thickness, we used:

$$\frac{dH}{dt} = \frac{1}{\rho_i L_i}\left(\frac{T_w - T_a}{\frac{1}{k} + \frac{H}{\lambda_i} + \frac{h}{\lambda_s}} - F_w\right) \tag{4}$$

every 6 hr to grow the sea ice at each grid cell.

F_w most often describes the heat flux from the warmer ocean to the colder ice, as the seawater below the ice either retains heat from the mixed layer in summer or receives heat from deeper waters (Petrich & Eicken, 2017). Negative values of F_w are sometimes observed in nearshore locations such as McMurdo Sound when seawater from ice-shelf cavities rises to the surface and experiences pressure-induced supercooling (Langhorne et al., 2015). F_w is highly spatially and temporally variable, with typical Antarctic values in the 0–20 W m^{-2} range but reaching hundreds of W m^{-2} during short, extreme events (Ackley et al., 2015; Heil et al., 1996; McPhee et al., 1996, 1999; Wilson et al., 2019). In our idealized model, F_w was held constant in the absence of a circumpolar data set for F_w and in lieu of more complicated parameterizations (e.g., McPhee, 1992; Wilson et al., 2019). All parameter values used for ice growth and for the ice algal habitat analysis are listed in Table 1.

At the beginning of each day, the sea ice was moved according to the ice motion vectors, and instances of divergence or convergence were reconciled based on the sea ice concentration. At time t, the sea ice concentration that can be explained in a given grid cell by ice motion, $c_{t_{motion}}$, was a combination of the ice from the previous day, c_{t-1}; the ice that has moved in from neighboring grid cells, c_{in}; and the ice that has exited the grid cell, c_{out}:

$$c_{t_{motion}} = c_{t-1} + c_{in} - c_{out}. \tag{5}$$

All of the values above are expressed in terms of sea ice concentration (0–100%).

$c_{t_{motion}}$ was compared to the sea ice concentration measured by passive microwave remote sensing, c_t, as the "true" value. When $c_{t_{motion}} > c_t$, ice converged at the grid cell. The ice thickness H_t was then an average of H_{t-1} of the contributing grid cells, weighted by their relative contributions to the sea ice concentration. Note that the weighted average in convergent cases means that the model is not volume-conserving. When $c_{t_{motion}} < c_t$, ice diverged from the grid cell. New ice was added to the grid cell at concentration $c_t - c_{t_{motion}}$ and given a thickness of 0.20 m (Saenz & Arrigo, 2014). H_t was calculated via weighted average, as in the convergent case, but with the addition of the new ice.

Because satellite-based sea ice concentrations were used to determine cases of convergence or divergence, the modeled sea ice cover always matched remotely sensed sea ice extent, timing, and distribution, including the formation of polynyas. The bottom ice melt date was set at each grid cell as the day after maximum ice thickness was reached (up through 31 January), at which point it was assumed that the algae slough off the bottom of the ice (Figure 1d).

2.1.2. Ice Thickness Initialization

Sea ice thickness was initialized on the date of the 2003 summer minimum (17 February) using an approximation modified slightly from Arrigo et al. (1998) that relates ice thickness and sea ice concentration. This is the first summer minimum for which estimates of snow depth from the chosen remote sensing product (Section 2.3) are available. Grid cells with ice concentrations above 80% had 1.28 m ice, grid cells with concentrations of 15% had 0.53 m ice, and concentrations in between were linearly interpolated. Ice concentrations below 15% were initialized as having no ice, as 15% is a commonly used threshold for measures of sea ice extent and was used as such in this study. Sea ice growth was spun up for 1 year (i.e., our first year of habitat analysis is 2004) and run continuously through the end of the time series.

2.1.3. Ice Thickness Validation

Sea ice growth was validated with in situ ice thickness measurements from the Antarctic Sea Ice Processes and Climate (ASPeCt) program (Worby et al., 2008). We were not able to exactly match the dates of ASPeCt

measurements, which span 1980–2005, and our modeled ice thicknesses, which span 2004–2019. We did match the locations and the day of the year with our model results for a total of 20,585 validation points from ASPeCt matched with 265,177 points from our model. For further analysis, we divided the months into four seasons: austral summer (December–February), fall (March–May), winter (June–August), and spring (September–November).

2.2. Ice Algal Habitat Assessment Parameters

For the ice algal habitat assessment, photophysiology parameters were adjusted to fit Antarctic ice algae—specifically, the maximum photosynthetic rate, P^*_{max}; the slope relating irradiance and photosynthetic rate before light saturation, α^*; and respiration, R^* (Table 1). Parameters were tuned slightly so that a standard run produced average spring production rates around 50 mg C m^{-2} d^{-1} from a median integrated Chl*a* of 43 mg m^{-2} (Arrigo, 2017) and a C:Chl*a* ratio of 35. Tuning resulted in standard run values of P^*_{max} = 0.64 g C g^{-1} Chl*a* m^{-2} h^{-1} and α^* = 0.062 g C g^{-1} Chl*a* h^{-1} [μmol photons m^{-2} s^{-1}]$^{-1}$, which are above the average values—but well within the overall ranges—reported in van Leeuwe et al. (2018) for algae in Antarctic pack ice. R^* was set to 13% of P^*_{max} to match the mean ratio of R^* to P^*_{max} in Trenerry et al. (2002).

2.3. Input Data

For input data, we used a combination of reanalysis and remote sensing data. Notably, we used a microwave radio-metry product recently developed by Shen et al. (2022) that estimates snow depths on Antarctic sea ice, which have historically been difficult to measure. Their algorithm incorporates lower frequency channels from the Advanced Microwave Scanning Radiometer for EOS and its successor (AMSR-E and AMSR-2) to improve snow depth estimation from June 2002 through May 2020 (daily, 25 km; Shen & Ke, 2021) when compared to the algorithms of Comiso et al. (2003) and Markus and Cavalieri (1998). Occasional days (<15 days total in our time series; never more than 7 days in a row) were missing from the snow depth data product; we linearly interpolated between the neighboring dates that had snow depth data. There were also some spatial gaps/missing grid cells in the snow depth data, presumably due to clouds or other remote sensing limitations. We similarly linearly interpolated between dates up to 7 days apart, and any remaining holes were filled with the value from the nearest-neighbor grid cell on the same date.

All other forcing data, describing atmospheric and sea ice conditions, did not require interpolation: (a) atmospheric conditions from the National Centers for Environmental Prediction/National Center for Atmospheric Research (NCEP/NCAR) Reanalysis Project 1 (4× daily, 2.5° resolution; Kalnay et al., 1996) and the National Aeronautics and Space Administration Ozone Record (daily, 1° resolution; https://ozonewatch.gsfc.nasa.gov), (b) sea ice concentrations from the National Oceanic and Atmospheric Administration/National Snow and Ice Data Center (NOAA/NSIDC) Climate Data Record of passive microwave sea ice concentration (Version 4, daily, 25 km resolution; Meier et al., 2021), and (c) the Polar Pathfinder sea ice motion vectors (Version 4, daily, 25 km resolution; Tschudi et al., 2019). All data were regridded to the 25 km Equal-Area Scalable Earth (EASE)-Grid South used for the sea ice motion vectors. Aside from filling missing days of snow depth data, input data were not temporally interpolated. That is, most forcing data were prescribed daily, except for NCEP/NCAR atmospheric conditions (every 6 hr, defining the ice model time resolution) and calculated sun angle (hourly, allowing habitat estimates every 3 hr).

2.4. Analysis and Statistics

The habitat assessment is expressed as the proportion of each 25 km grid cell that was habitable for ice algae each day during the potential growing season, defined as June–January to capture late winter, spring, and early summer blooms. For reference, monthly examples from 2005 to 2006 are provided in Figure S1 in Supporting Information S1. Specifically, potential habitat in a grid cell was quantified as a proportion because snow was given a log-normal distribution within each grid cell to account for its high spatial variability (Arrigo et al., 1998). Because each grid cell had a daily proportion of habitat that ranged from 0/9 to 9/9, we report the metric of habitat-days (km^2 d) that is defined in Lim et al. (2022) to integrate spatially and temporally over the entire ice season. We also use the metric of normalized habitat-days (d), which can be thought of as the spatially averaged duration of ice algal habitat, to describe ice algal habitat for each grid cell, for the entire Antarctic, or when divided into latitudinal bands or geographic sectors (Figures 1g and 1h; Arrigo et al., 2008). Text S1 in Supporting Information S1 contains a more detailed explanation of the habitat-days metric.

Aside from melt date and the date of ice advance, which are singular metrics for each grid cell each year, we often report environmental variables as means over the ice algal growing season (June–January). The first date on or after 15 February when the sea ice concentration in a grid cell is ≥15% is considered the date of ice advance in order to establish an annual metric, even though the ice edge can advance and retreat multiple times from the same grid cell during freeze-up. Parts of the EASE grid extend up to 37°S, so the data were first filtered to only include grid cells that have sea ice at some point during the growing season. For each grid cell, ice thicknesses and snow depths were then averaged for days with ice cover in a particular grid cell, while daylength, incident light, and air temperature were averaged for all days from June through January. The intent was to, as much as possible, separate the changes in sea ice presence/absence and timing from inherent changes in the other factors.

Trends in environmental data and in habitat-days over 16 years were estimated using the nonparametric Mann-Kendall Trend test, with modifications to account for possible serial correlation, and the accompanying Theil-Sen slope, as implemented in the pymannkendall package in Python (Hussain & Mahmud, 2019; Kendall, 1975; Mann, 1945; Sen, 1968; Yue & Wang, 2004). An alpha level of 0.05 was used for all statistical tests. Normalized habitat-days were tested for correlations using simple linear regressions (ordinary least squares) in Python's SciPy package (Virtanen et al., 2020) with several large climate modes: the SAM (Mo, 2000), the Southern Oscillation Index (SOI) from NOAA National Centers for Environmental Information (https://www.ncei.noaa.gov/access/monitoring/enso/soi), the Amundsen Sea Low (ASL; Hosking et al., 2016; https://climatedataguide.ucar.edu/climate-data/amundsen-sea-low-indices), and the Indian Ocean Dipole (IOD; Saji & Yamagata, 2003; https://psl.noaa.gov/gcos_wgsp/Timeseries/DMI). Correlations were tested with each index averaged over a year (January–December), the ice algal growing season (June–January), austral summer, fall, winter, and spring (seasons defined in Section 2.1.3). The various time frames were included to test potential lag effects and dampening periods within a year, while annual indices were also tested with offsets of up to 5 years in case of longer lag effects.

To investigate the impact of environmental forcings on Antarctic ice algal habitat, backward selection multiple linear regressions were run to explain normalized habitat-days between sectors (n = 16 years × 5 sectors) and individual grid cells ($n \approx$ 16 years × 35,000 grid cells for one combined regression and $n \approx$ 35,000 grid cells for regressions of individual years). Depending on the specific regression, explanatory variables were a subset of the mean daylength, mean incident light (Figure 1e), mean snow depth, mean ice thickness, date of ice advance (Figure 1f), melt date, SAM Index, and SOI. We report the results for regression analyses run using annual averages of the SAM index and SOI, but regressions run with seasonal means were comparable. The relative contribution of each explanatory variable was estimated using the lmg approach implemented in the relaimpo package in R (Grömping, 2006; Lindeman et al., 1980). Further descriptions of statistical analyses are in Text S2 in Supporting Information S1.

2.5. Uncertainty Calculation

Many characteristics of the snow-ice ecosystem are challenging to estimate or measure due to the complexity of the system and to the difficulties of working in the Antarctic. Thus, there is inherent error and uncertainty associated with the input data that force our ice algal habitat assessment. Of those, snow depth likely adds the most uncertainty to our habitat estimates, given both the limitations of snow depth estimation and validation (reviewed in part in Webster et al., 2018) and the high light attenuation by snow (Table 1; Perovich et al., 1986). The uncertainty in habitat-days for each year was calculated by uniformly adding or subtracting 0.14 m of snow to the Shen et al. (2022) snow depth estimate across the Antarctic, before application of the log-normal distribution. In cases when subtracting 0.14 m of snow resulted in a value ≤0 m, the snow depth was set to 0.001 m because changing from a snow-covered surface to bare ice would alter the specular reflection. The habitat-days estimates from the +0.14 m of snow (high snow, low habitat) and −0.14 m of snow (low snow, high habitat) runs are reported as ranges in parentheses following results from the control run. These ranges are conservative and represent extreme scenarios, as the Shen et al. (2022) snow depth estimates are unlikely to be uniformly high or uniformly low across the Antarctic.

2.6. Sensitivity Analyses

Sensitivity analyses were performed to determine how parameter values affected the habitat assessment. Parameters involved in light transmission and algal photophysiology, as well as F_w, were varied by ±50% for the year

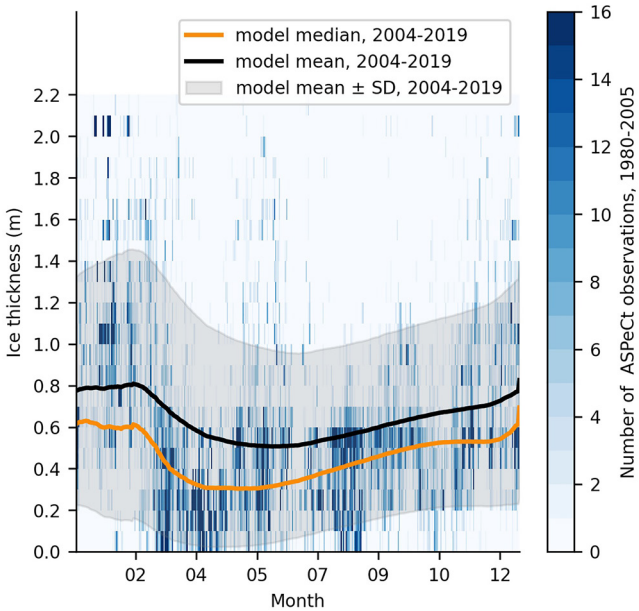

Figure 2. Yearly cycle of Antarctic sea ice thickness from all ASPeCt observations (n = 20,585) and the ice growth model.

2014, which was a year with a typical amount of ice algal habitat. In two additional treatments, the algal layer was moved from 0.05 m to (a) 1 m above the ice-water interface to simulate the addition of algae in the interior ice and (b) the snow-ice interface. No bottom ice algae were simulated in these treatments; that is, if the ice was less than 1 m thick, there was no habitat. We maintained bottom ice melt as the timing of bloom termination for lack of nutrient information, and thus both treatments should be considered rough approximations to assess the magnitude of the contributions by interior and surface ice to algal habitat.

3. Results

To provide an overview of the recent patterns in Antarctic ice algal habitat, we begin by validating the thermodynamically grown sea ice thickness, an essential input to the ice algal habitat assessment. We then describe important environmental conditions and their corresponding trends before reporting the resulting ice algal habitat on a range of spatial scales: as a circumpolar whole, by sector, by latitudinal band, and by 25 km grid cell. Lastly, we detail how the assessment responds to different parameterizations.

3.1. Ice Thickness Validation

Modeled Antarctic sea ice was generally thin, with an annual average of 0.68 ± 0.10 m during 2004–2019 (circumpolar mean ± standard deviation, n = 16 years). Sea ice thicknesses on the dates of the summer minimum and winter maximum ice extent averaged 0.81 ± 0.07 and 0.62 ± 0.03 m, respectively (n = 16 years). The sea ice thickness model showed no drift over its 16-year run, but did produce some interannual variability (Figures S2–S4a in Supporting Information S1). These simulated thicknesses are similar to the long-term means of the ASPeCt data set, which reported an average of 0.87 m for all sea ice, including ridges, and 0.62 m for level, undeformed ice (Worby et al., 2008). If we take the output of the fifth Coupled Model Intercomparison Project (CMIP5) multi-model ensemble mean and divide the 1979–2005 mean annual sea ice volume of 7.73×10^3 km^3 by the mean annual sea ice extent of 11.50×10^6 km^2, we arrive at a comparable 0.67 m thickness. However, comparison to a data-assimilating global ice-ocean model suggested that sea ice in the CMIP5 ensemble is too thin (Shu et al., 2015), and any model or remote sensing estimate of ice thickness remains uncertain.

The seasonal pattern of ice thickness from our idealized model (2004–2019) and from all ASPeCt observations (1980–2005) match well (Figure 2). The model simulated a higher frequency of thinner ice than the ASPeCt data (Figure 3), which is reasonable given a likely field sampling bias for thicker ice and because we do not account for ridging or rafting. In the summer, the frequency distributions of both modeled and observational data are shifted toward thicker ice that survives the melt season (Figure 3b). ASPeCt observations were generally distributed across sectors, and the Indian and Pacific sectors were well sampled in all seasons (Figure S4 in Supporting Information S1). The Bellingshausen-Amundsen sector only had winter and spring observations. Summer and fall observations in the Ross and Weddell Seas were generally closer to the continent than winter and spring observations. Because areas with thick ice were not sampled as frequently from June to November, the seasonal cycle captured by the ASPeCt compilation may be biased. Indeed, the Massachusetts Institute of Technology general circulation model (MITgcm) simulated a seasonal cycle with a maximum ice thickness in November (Holland et al., 2014) in contrast to the end of December or February peak in our model and in the ASPeCt data (Figure 2)—although it should be noted that ice thickness estimates from the MITgcm were larger than those from the Ice, Cloud, and Land Elevation Satellite in November (Holland et al., 2014).

The idealized model produced thick ice (>1.5 m) in areas of known multiyear ice accumulation in the Weddell Sea and between the western Ross Sea and the Amundsen Sea (Figure 1a and Figure S3a in Supporting Information S1; Meiners et al., 2012). These areas also tended to have higher interannual variability in sea ice thickness (Figure S4a in Supporting Information S1). Regionally, the model overestimated ice thickness in the Ross Sea (Figure S5c in Supporting Information S1), which may be attributed to particularly rapid movement of sea ice offshore (Comiso et al., 2011; Holland & Kwok, 2012). This movement may increase the relative importance of

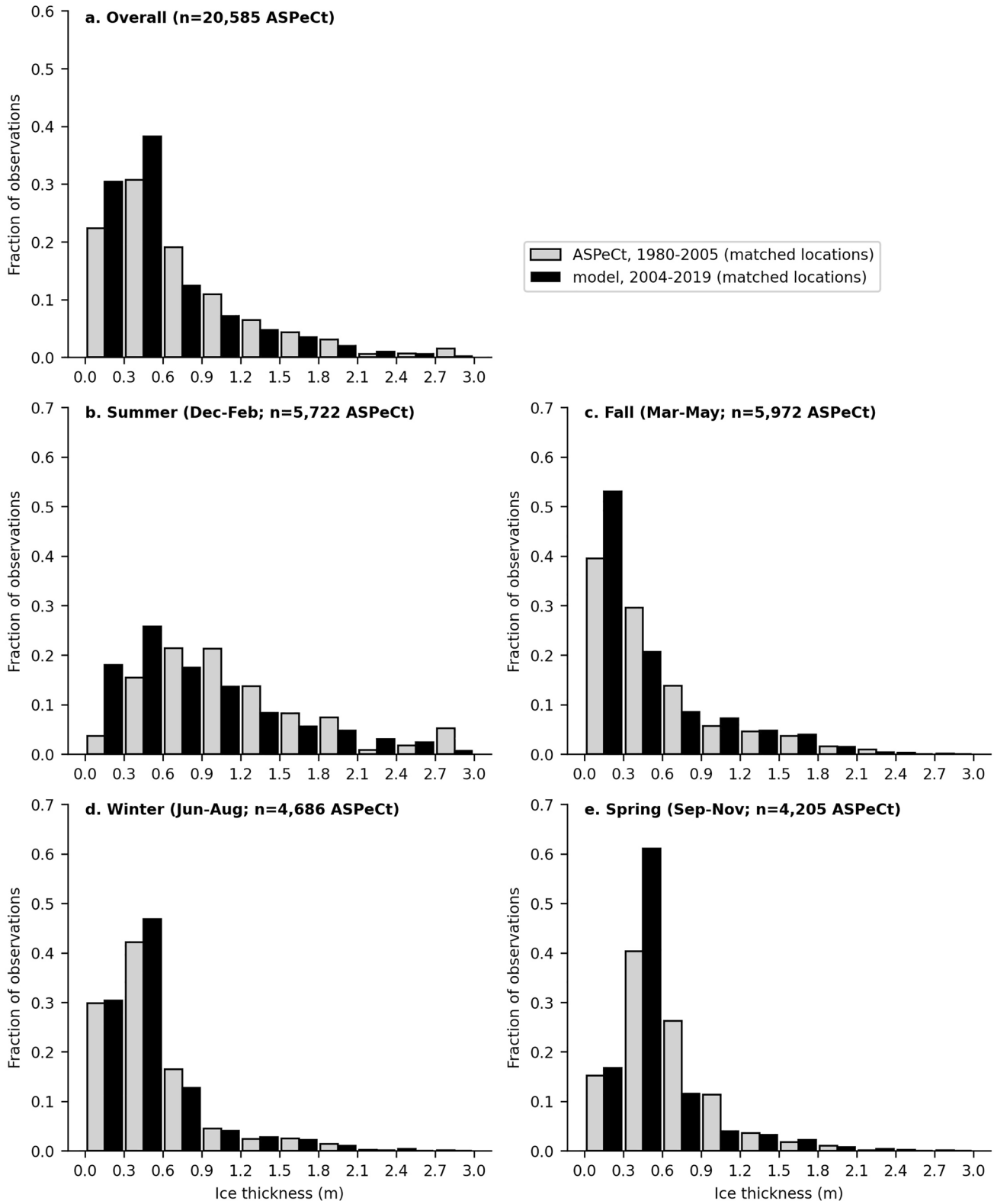

Figure 3. Frequency distribution of in situ ASPeCt data and modeled ice thicknesses, (a) year-round and (b–e) by season. Note that the sample size, *n*, refers to the number of ASPeCt observations, which can be multiplied by 16 to get the approximate number of matched model estimates (one per year of the model).

some sea ice dynamics that are not represented in our model; in a study that compared the thermodynamic and dynamic forcings of a coupled ocean-sea ice model, the Ross Sea was the only sector where wind stress surpassed thermodynamics as the main driver of sea ice extent (Kusahara et al., 2019). It is also possible that the rapid ice floe motion in the Ross Sea is not well captured in the Polar Pathfinder product. With the understanding that our sea ice model is by definition limited but makes use of newly improved snow depth estimates—which are considered one of the biggest limitations to accurately simulating thermodynamic ice growth (Notz, 2012)—we now proceed to use our modeled ice thickness as an informative tool to diagnose ice algal habitat.

3.2. Environmental Inputs

To set the context of the Antarctic sea ice environment, variables with the potential to affect the extent and duration of ice algal habitat are presented as averages for June–January (the months for which we ran the habitat assessment). The exceptions are the maximum ice extent, date of ice advance, and melt date, which are quantified using a single metric that applies for the entire year. Using 2005 as an example year (for comparison with Saenz & Arrigo, 2014), sea ice froze starting from the Antarctic landmass and continuing northward, as evidenced in the later ice advance dates at lower latitudes (Figure 1f). Air temperatures also showed a latitudinal pattern, with the coldest air along the Antarctic continental margins (Figure 1c). In contrast, bottom ice melt dates did not follow a latitudinal pattern but were highly patchy (Figure 1d). The mean snow depth was 0.28 ± 0.02 m (n = 16 years) but was occasionally ≥0.80 m in winter. Snow depths tended to be more evenly distributed across the Antarctic ice pack than ice thicknesses (Figure 1b). Maps of the long-term means and interannual standard deviation of environmental inputs during 2004–2019 are presented in Figures S3 and S4 in Supporting Information S1. In most regards, the spatial patterns in the long-term means closely resemble those of 2005, with the exception of melt date, which has a high interannual variability at many grid cells such that the patchiness visible in 2005 (Figure 1d) is smoothed out over the time series (Figure S3d in Supporting Information S1).

We only report trends (for environmental variables and ice algal habitat) that are statistically significant. Winter sea ice extent in the Antarctic decreased during 2004–2019, although embedded in this trend is an increase and then drop off after 2016 (Figure 4a). The circumpolar-averaged air temperature decreased by 0.5°C decade^{-1} and the average snow depth decreased by 0.01 m decade^{-1} (Figures 4b and 4c). While both changes would have altered the thermodynamic balance of the sea ice and therefore vertical growth and melt, the effects were too small to be statistically distinguished in the average ice thickness, date of ice advance, or melt date, which all showed no trend (Figures 4d–4f). At this rate of change, the thinning snow cover may have altered light transmission but likely not ice thickness. Average incident PAR showed a relatively minor decrease of 1.2% over the 16-year study (Figure 4g). Circumpolar and regional means and trends for environmental inputs are reported in Tables S1, S2, and S4 and mapped in Figure S7 in Supporting Information S1. There were often contrasting positive and negative trends between different regions—or within a single region—that compensate at the circumpolar scale. For example, the northern Ross Sea featured a strong increase in sea ice thickness, while the Ross Sea off Oates Land featured a strong thinning (Figure S7c in Supporting Information S1).

3.3. Ice Algal Habitat

We examined the extent and duration of Antarctic ice algal habitat at several spatial scales. At the circumpolar scale between 2004 and 2019, an average of 92 ± 2 (uncertainty range = 31–100)% of Antarctic sea ice experienced at least 7 habitat-days each year, and 81 ± 3 (13–94)% of ice experienced at least 14 habitat-days. Average normalized habitat-days for the entire Antarctic was 38.1 ± 2.3 (7–65) d. At a growth rate of 0.22 d^{-1} (estimated growth rate at light level $E_k = \frac{P_{\max}}{\alpha}$ using the parameters in Table 1), 14 days would allow the starting population to grow to over 20 times its starting biomass. There was no trend in habitat-days (km^2 d decade^{-1}) summed across the entire ice pack, and the drop in sea ice extent during 2016–2019 did not negatively affect the aggregate amount of ice algal habitat. When adjusted for the decreasing maximum ice extent over time, there was an increase in normalized habitat-days of 2.6 days during 2004–2019 (Figure 4h, Table S3). As there was no change in the circumpolar-averaged dates of the ice algal bloom start (data not shown) or finish (Figure 4f), the increase in normalized habitat-days between 2004 and 2019 suggests that there was an increase in the fraction of the sea ice area that was habitable, rather than a lengthening of the ice algal season. Lastly, there was no correlation between the circumpolar number of normalized habitat-days with the SOI, ASL, or IOD at any time scale or when lagged. The circumpolar number of normalized habitat-days was positively correlated with the 3-month spring index for the SAM (R = 0.55), but not the annual or the 8-month growing season index.

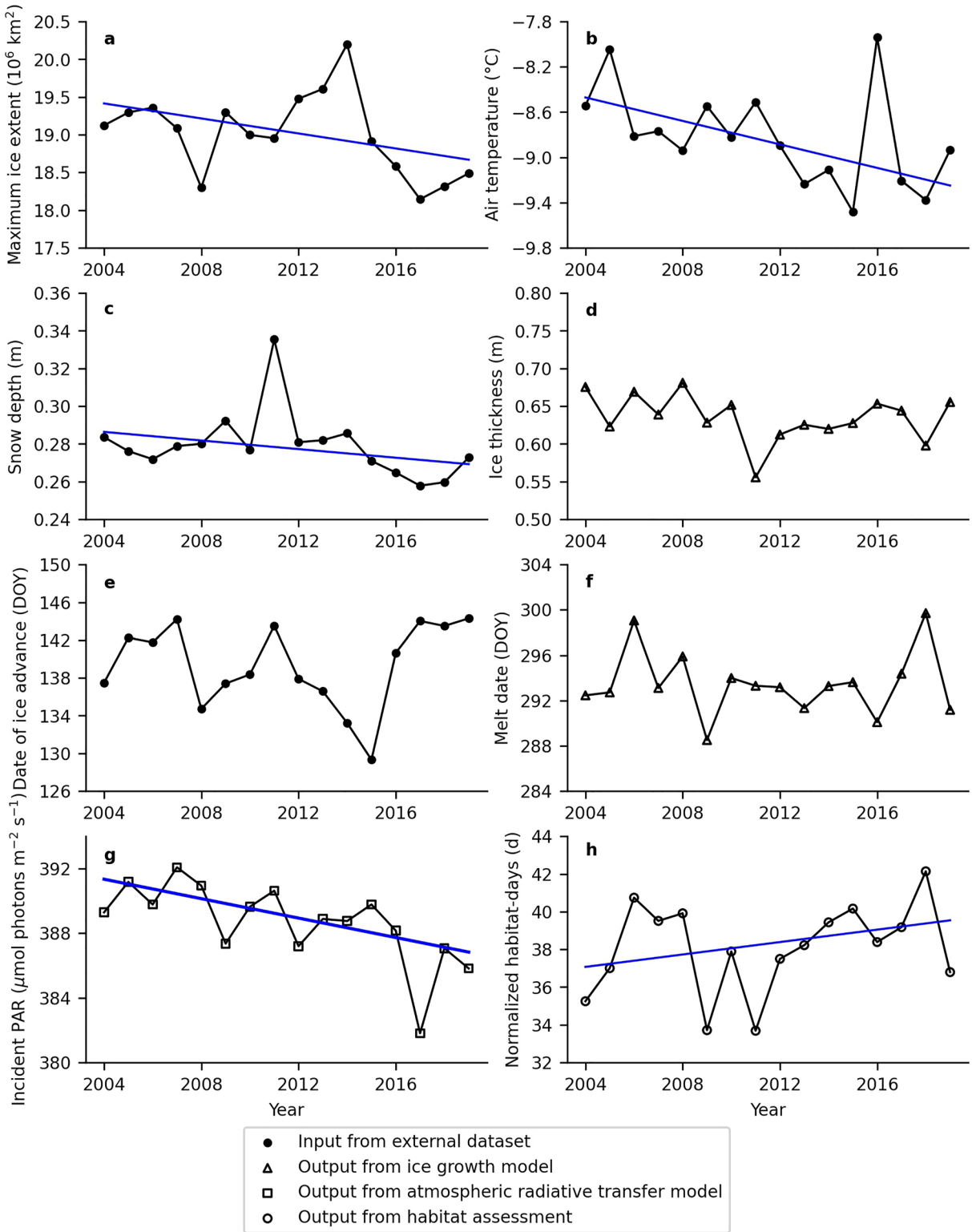

Figure 4. Trends in ice algal habitat assessment inputs and outputs: average circumpolar (a) maximum ice extent, (b) air temperature, (c) snow depth, (d) ice thickness, (e) date of ice advance as day of the year (DOY), (f) bottom ice melt date, (g) downwelling incident photosynthetically active radiation (PAR), and (h) normalized habitat-days. (b–d) and (g) are averaged June–January, while (a, e, f, and h) are annual metrics. Standard deviations around the circumpolar means are reported in Table S4. Trend lines indicate a significant trend based on a Mann-Kendall Trend test with an accompanying Theil-Sen slope estimate.

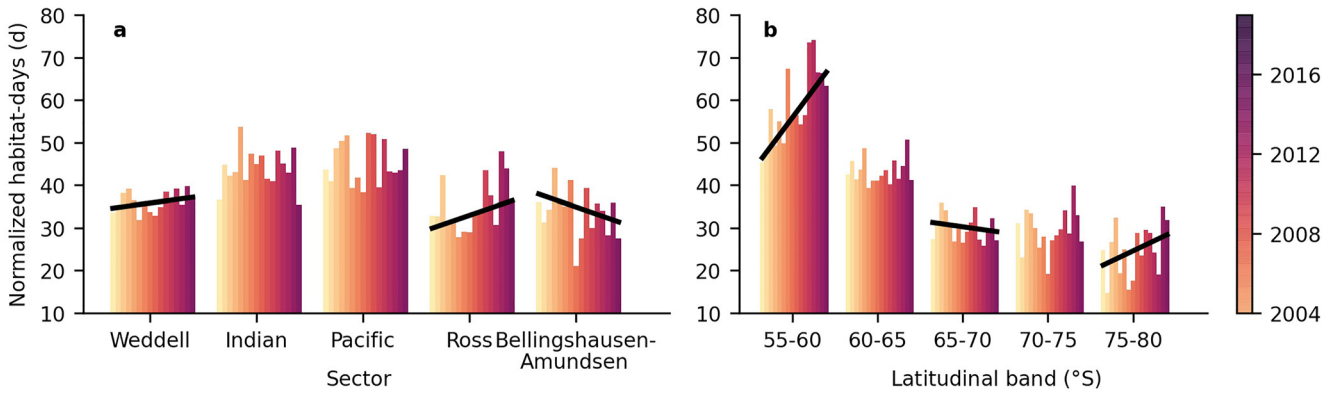

Figure 5. Time series of normalized habitat-days calculated for (a) sectors and (b) latitudinal bands (see Figure 1h). Black lines indicate a significant trend based on a Mann-Kendall Trend test with an accompanying Theil-Sen slope estimate.

Geographic sectors fell into two statistically distinct groups with respect to their number of normalized habitat-days each year. The Ross, Bellingshausen-Amundsen, and Weddell sectors averaged 35.3 ± 5.9 (6–72), 33.5 ± 5.6 (7–48), and 36.1 ± 2.3 (5–60) days, respectively, while the Indian and Pacific sectors averaged 44.0 ± 4.4 (7–76) and 45.5 ± 4.8 (10–68) days, respectively (n = 16 years, ANOVA and Tukey's test, Figure 5a, Table S3). On the regional scale, the only correlation between a climate mode and normalized habitat-days was with the spring SAM in the Indian sector ($R = 0.67$). The Ross and Weddell sectors exhibited positive trends in normalized habitat-days during 2004–2019, while the Bellingshausen-Amundsen was the only sector with a negative trend. In the regional multiple linear regression, 28.9% of the variation in normalized habitat-days was explained by snow depth, 19.2% by melt date, 17.2% by ice thickness, 9.3% by incident light, and 7.4% by the date of ice advance (Table S5).

When divided into 5° latitudinal bands, sea ice showed a distinct nonlinear decrease in the number of normalized habitat-days when moving from north to south (Figure 5b). Latitudinal bands, especially the northernmost and the southernmost, also had fairly high interannual variability, with standard deviations of normalized habitat-days up to 8.7 days (n = 16 years). As with sectors, there were mixed temporal trends in normalized habitat-days between bands, with the fastest increase of 13.4 days decade^{-1} observed in the 55°–60°S band. There was also a slower increase of 4.8 days decade^{-1} in the 75°–80°S band and a decrease of 1.4 days decade^{-1} in the 65°–70°S band.

However, ice algal habitat in a given year clearly varied on a much finer spatial scale than that captured by binning data into sectors or latitudinal bands (Figure 1h). Indeed, the standard deviations of normalized habitat-days for grid cells within a single sector spanned 9–26 days (uncertainty range = 3–35; n = 3,500–11,800 grid cells depending on the sector). The location of highly habitable ice varied greatly between years, such that the long-term mean of normalized habitat-days was more spatially smooth (Figure S3g in Supporting Information S1). Trends in normalized habitat-days were also patchy and frequently contrasted within the same sector (Figure 6b). Therefore, we examined the patterns in and drivers of ice algal habitat on a 25 km scale, the highest resolution of our input data. A visual comparison clearly indicates that, when compared to the various input factors, the spatial pattern of normalized habitat-days (Figure 1g) most closely resembles that of the sea ice melt date (Figure 1d) in 2005. Moreover, the spatial pattern of the trends in normalized habitat-days between 2004 and 2019 were strikingly similar to those in the sea ice melt date (Figure 6 and Figure S7 in Supporting Information S1). A multiple linear regression combining all 16 years of individual grid cell data showed that 45% of the spatial and interannual variation in normalized habitat-days was explained by melt date (Table S5). Other factors—daylength, SOI, incident light, snow depth, ice thickness, and the date of ice advance—each explained ≤3%. When grid cell by grid cell regressions were run for each year, melt date and snow depth both became larger contributors to the R^2 over time, while ice thickness became a smaller contributor (Figure 7, Table S5).

3.4. Sensitivity Analyses

In general, the sensitivity analyses revealed that the habitat assessment was not sensitive to most parameters. All parameter changes of ±50% resulted in a <50% change in circumpolar habitat-days (Table S6). In fact, the response in normalized habitat-days was typically much less (<28%), except when the diffuse attenuation coefficient of dry snow was decreased by 50%, causing a 48.2% increase in normalized habitat-days. Moving the

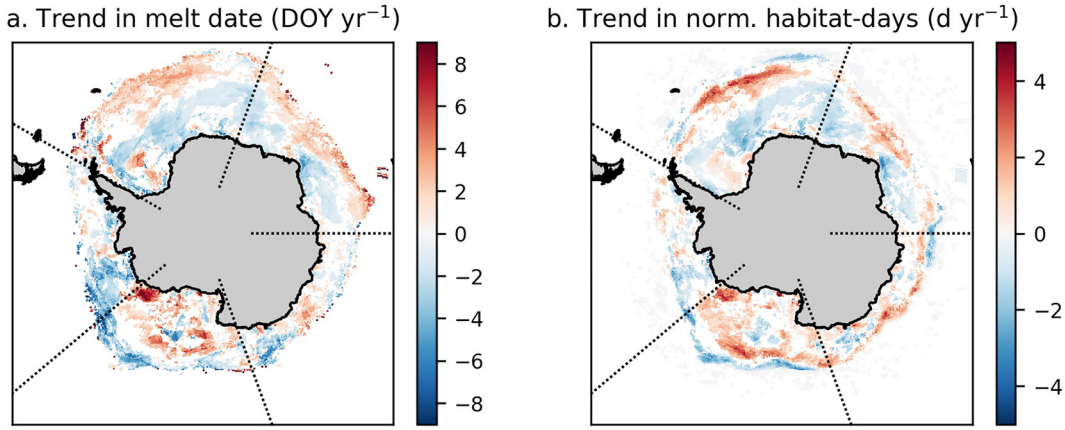

Figure 6. Maps of (a) trends in bottom ice melt date and (b) trends in normalized habitat-days during 2004–2019. Only grid cells with significant trends, based on a Mann-Kendall Trend test with an accompanying Theil-Sen slope estimate, are shown.

algal layer to 1 m from the ice-water interface to simulate interior ice had minimal effect (4.2% increase), while moving it to the snow-ice interface increased normalized habitat-days by 41.4%. Knowing that bottom ice melt date explained the most variation in normalized-habitat days, we examined the sensitivity analysis for F_w, which directly contributed to the thermodynamic balance of the sea ice: a 50% increase in F_w resulted in ice that was 0.16 m thinner and melt dates that were 11.8 days earlier on average for a 4.8 days (13.5%) decrease in circumpolar normalized habitat-days (Table S6). A 50% decrease in F_w caused 0.08 m thicker ice on average, 11.1 days later melt dates on average, and a 2.4 days (6.9%) increase in normalized habitat-days.

4. Discussion

The major goal of this study was to investigate the recent status, trends, and variability in Antarctic bottom ice algal habitat and its environmental drivers. Below, we discuss our findings that: (a) Antarctic sea ice is widely habitable and is more so than Arctic sea ice; (b) potential habitat did not respond to the 2016–2019 drop in sea ice extent and instead increased in concentration within grid cells; and (c) high spatial variability in potential habitat reveals that bottom ice melt date is the dominant environmental driver. We conclude by leveraging our understanding of the factors currently controlling Antarctic ice algal habitat to predict its future sensitivity to environmental change.

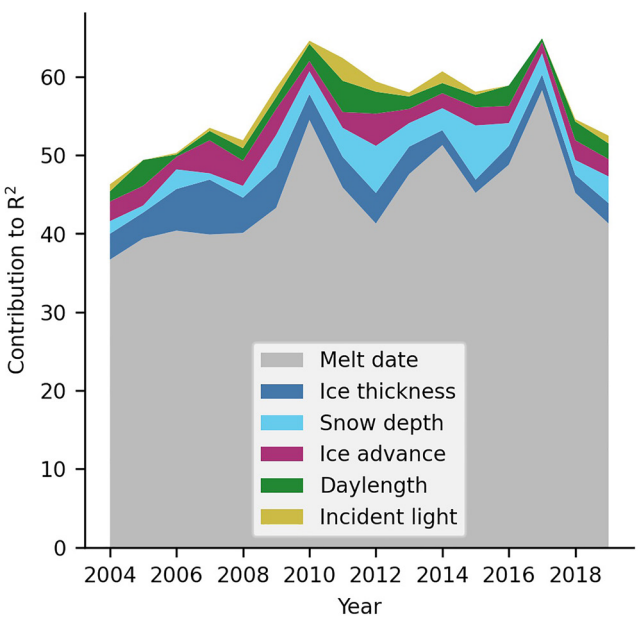

Figure 7. Time series of the relative importance of various input factors, reported as their estimated contribution to the R^2 in annual grid cell by grid cell multiple linear regressions. Bottom ice melt date and the date of ice advance are annual metrics, while the remainder are June–January means.

4.1. Status of Ice Algal Habitat

With 92% of Antarctic sea ice reaching 7 habitat-days and 81% reaching 14 habitat-days on average, the vast majority of the ice pack transmitted enough light to support bottom ice algal communities. Field data show that most ice algal blooms last at least 14 days, although data from sea ice camps are largely restricted to a few sites on landfast sea ice (Archer et al., 1996; Arrigo et al., 1995; Cota & Sullivan, 1990; Grossi et al., 1987; Grotti et al., 2005; Guglielmo et al., 2000; Lazzara et al., 2007).

Compared to the Arctic Ocean, the Antarctic has a larger extent, proportion, and duration of ice algal habitat. In the Arctic, only 48%–66% of sea ice reached ~7 habitat-days during 1985–2018 and, on average, Antarctic sea ice supports algal growth for twice as long as Arctic sea ice (38.1 vs. 18.6 normalized habitat-days; Lim et al., 2022). One likely reason for this difference is that the Arctic has a greater amount of thick, multiyear ice (Kwok, 2018) that attenuates incoming light; the mean ice thickness in the

Arctic is more than twice that of the Antarctic (Lim et al., 2022). Sea ice also exists at higher latitudes in the Arctic, resulting in an average incident PAR over Arctic sea ice that is 19% lower than that of the Antarctic (Lim et al., 2022). However, model estimates of annual primary production in Antarctic (23.7–35.7 Tg C year^{-1}) and Arctic (10–36 Tg C year^{-1}) sea ice are comparable because the per-meter rates of production are higher in the Arctic (Arrigo, 2017; Arrigo et al., 1997; Deal et al., 2011; Dupont, 2012; Jin et al., 2012; Saenz & Arrigo, 2014).

To understand the positive correlation between the spring SAM and normalized habitat-days—which was significant only on the circumpolar scale and in the Indian sector—we investigated associations between the SAM and other environmental variables. There was a positive correlation between the spring SAM and melt date on the circumpolar scale ($R = 0.61$) and in the Indian sector ($R = 0.55$). During a positive SAM, surface air temperatures south of 60°S are generally lower than normal, aside from some warming over the Antarctic Peninsula (Fogt & Marshall, 2020; Marshall, 2007). These lower temperatures are likely to delay the bottom ice melt and thus extend the ice algal season. A negative SAM usually features the opposite conditions—higher surface air temperatures (Fogt & Marshall, 2020; Marshall, 2007) and earlier melt dates—which lead to fewer habitat-days.

In this study, we focus on ice algal habitat in the bottom 0.05 m of the sea ice in spring because it is easier to represent within the limitations of remote sensing and model data. We cannot know when algal habitat in the upper ice would end without including nutrient concentrations and an algal pool in our model. Our chosen approach almost certainly underestimates ice algal habitat in the Antarctic, as surface and internal communities account for 29.2% and 31.4%, respectively, of integrated Chl*a* in compiled ice core data (Meiners et al., 2012). Spatially, surface flooding, which promotes surface communities, may affect 5%–55% of sea ice, with the highest percentage of flooded ice in the spring (Saenz & Arrigo, 2014); in the Weddell Sea, a region with thick, heavy snow, field measurements in winter found that 13%–30% of the sea ice was flooded (Wadhams et al., 1987). Wet snow or snow-ice also transmits more light than dry snow, though this may be offset by light absorption by algae (Perovich, 2002). Our sensitivity analyses indicated that potential habitat could increase substantially if we included the snow-ice surface; less so with internal layers. The increased habitat in the upper sea ice may not scale directly to primary production (Saenz & Arrigo, 2014) and ecosystem impacts, however, and the dominant ice algal dynamics are likely captured here.

4.2. Trends

With regards to temporal trends, air temperatures over Antarctic sea ice decreased by 0.5°C decade^{-1} during our study period, but the direct impacts of this decrease were minimal, as cooler temperatures did not translate to changes in ice thickness, melt date, or the date of ice advance. The 1.2% decrease (2004–2019) in incident PAR (400–700 nm) over sea ice from the atmospheric radiative transfer model forced by observations and reanalysis data is in approximate agreement with a 0.2% decrease (1987–2017) in 200–5,000 nm incident irradiance from the International Satellite Cloud Climatology Project, likely driven by changes in cloud cover (Pinkerton & Hayward, 2021). Perhaps the most notable trend in the input data was a decrease in average snow depth (Shen et al., 2022) during the ice algal season which, although small compared to the interannual variability, declined at a rate (−0.01 m decade^{-1}) more than three times that of Arctic snow depth (−0.003 m decade^{-1}; Lim et al., 2022). To our knowledge, there are no other medium- to long-term products of snow depth on Antarctic sea ice for comparison (Webster et al., 2018). Given the course (2.5°) resolution of the atmospheric input data (including air temperatures) and our use of circumpolar averages, these temporal trends in the Antarctic sea ice environment are meant as overviews of highly variable system, aspects of which have been documented by many other studies (e.g., Hobbs et al., 2016; Matear et al., 2015).

Normalized habitat-days increased between 2004 and 2019 because a greater proportion of each grid cell became potential habitat for ice algae. The closest comparison for our habitat estimates is that of Pinkerton and Hayward (2021), who calibrated a time series of remotely sensed incident light and sea ice concentration with outputs from the baseline run of a sea ice ecosystem model (Saenz & Arrigo, 2014) to estimate trends in ice algal production (1987–2017). They found that circumpolar primary production increased over time. Although we did not estimate production in our study, the increases in ice algal habitat could support increased production. In addition, because potential habitat became more "concentrated" in smaller areas of ice, the 2016–2019 drop in sea ice extent did not negatively impact total ice algal habitat. Thinning snow, which was the most important input variable in the regional regression, is one likely explanation for sea ice grid cells becoming more habitable. A smaller mean snow depth at any given grid cell allows a higher proportion of sea ice within the cell to transmit

enough light to support ice algal growth. An additional factor may be bottom ice melt date, which played a large role in controlling the small-scale variability in normalized habitat-days as discussed below.

4.3. Spatial Variability

More striking than the temporal trends found in this 16-year study was the horizontal patchiness of Antarctic ice algal habitat (Figures 1g and 6b). Other studies have recognized that ice algal habitat is highly variable on scales ranging from meters to hundreds of kilometers (reviewed in Cimoli et al., 2017), and our habitat assessment provides further evidence that this is the case across the Antarctic at the 25 km scale. Increases in ice algal habitat were strongest in the eastern Ross Sea and offshore in the Weddell Sea (Figure 6b), which loosely correspond to the areas with the largest increases in ice algal production in Pinkerton and Hayward (2021): East Antarctica, the western Ross Sea, and the Weddell Sea. Importantly, the spatial patterns in ice algal habitat were not consistent within geographic sectors nor latitudinal bands, and aggregating data over these large areas is likely to mask key information about ice algal habitat and its environmental drivers. For example, our regression analysis indicated that snow depth explained the most variation (28.9%) in regional habitat and was fairly closely followed by melt date (19.2%) and ice thickness (17.2%). However, the grid cell by grid cell regression told a different story, where melt date explained by far the most variation in habitat (45.0%). Further considering how the map of melt date strongly resembles the map of normalized habitat-days—and the same with the trends in each—we propose that melt date was the most important driver of ice algal habitat variability in 2004–2019. Although localized shifts to earlier and later melt dates balanced at the circumpolar scale to produce no overall trend, they could still notably affect the circumpolar habitat estimates because the relationship between changes in melt date and changes in ice algal habitat is not 1:1. That is, a 1 day shift in melt date does not necessarily equate to a 1 day increase/decrease in normalized habitat-days. In the F_w sensitivity analysis, a 1 day shift in the circumpolar-averaged melt date resulted in a 0.2–0.4 days change in normalized habitat-days because the effects of changes in melt date depend on complex interactions with all other environmental factors. For example, a shift to an earlier melt date only results in fewer habitat-days if enough light is transmitted through the snow and ice to support algal growth, such that a potential bloom is terminated early. Increasing F_w shifts melt dates earlier but also thins the sea ice, with the latter potentially dampening the effect of the former on net algal habitat. Thus, when we characterized Antarctic ice algal habitat at a smaller scale, rather than using sectors or latitudinal bands, we saw that melt date has a distinct, sizable, and nonlinear effect on circumpolar habitat estimates.

4.4. Implications

We can use the recent record of Antarctic ice algal habitat and its response to environmental conditions to predict its vulnerability to future changes. Due to the relatively short satellite record of snow depth, it is too early to disentangle the effects of climate change on Antarctic ice algal habitat from patterns due to climate oscillations and normal interannual variability. Studies estimate that 34–40 years of data are necessary to distinguish climate change trends in phytoplankton Chl*a* and primary production in the Southern Ocean (Del Castillo et al., 2019; Henson et al., 2010), and it is likely that the time series for ice algal habitat would need to be of a similar length. However, both the interannual and spatial variability of ice algal habitat during 2004–2019 demonstrate that Antarctic ice algal habitat has been and will likely continue to be quite sensitive to changes in snow depth and atmospheric conditions. In particular, bottom ice melt date as the dominant (and an increasingly important) factor explaining spatial patterns in habitat suggests that the Antarctic ice algae are likely to be affected by the conditions controlling vertical sea ice growth, especially air temperature, ocean heat flux, and sea ice motion (driven by winds and surface currents). CMIP6 predicted that air temperatures over the Southern Ocean will increase between 1.5°C and 6°C by 2100, depending on the latitude and forcing scenario (Bracegirdle et al., 2020), and this magnitude of warming is likely to have a more observable impact on ice algal habitat than the net −0.8°C change in our study. Ocean heat fluxes are also likely to increase, given many projections of increased Southern Ocean heat content (Cheng et al., 2022). Either change could feasibly cause bottom sea ice to melt earlier and terminate ice algal blooms sooner each year. Given its increasing importance during our 16 years study, snow depth may be a second influential factor on future ice algal habitat. CMIP6 predicted increased precipitation rates over the Southern Ocean by 2100 (Bracegirdle et al., 2020), although snow accumulation on sea ice also depends on the duration and timing of the sea ice season. A thicker snow cover would attenuate more light, likely decreasing ice algal habitat.

Data Availability Statement

The habitat assessment code and output are available at https://doi.org/10.25740/jn797cv3253 (Lim et al., 2023). The citations for data used as inputs (e.g., snow depth, atmospheric reanalysis, sea ice motion, climate indices) are included directly in the text and references.

Acknowledgments
Thank you to the two anonymous reviewers for their feedback, which helped improve this work. We also thank Earle Wilson and Leif Thomas for discussing the ice model and validation. S.M.L. was funded by the National Science Foundation Graduate Research Fellowship Program Grant DGE-1656518 and a Stanford Graduate Fellowship (Ford Foundation Fellow).

References

Ackley, S. F., Xie, H., & Tichenor, E. A. (2015). Ocean heat flux under Antarctic sea ice in the Bellingshausen and Amundsen Seas: Two case studies. *Annals of Glaciology*, *56*(69), 200–210. https://doi.org/10.3189/2015AoG69A890

Archer, S. D., Leakey, R. J. G., Burkill, P. H., Sleigh, M. A., & Appleby, C. J. (1996). Microbial ecology of sea ice at a coastal Antarctic site: Community composition, biomass and temporal change. *Marine Ecology Progress Series*, *135*, 179–195. https://doi.org/10.3354/meps135179

Arrigo, K. R. (2017). Sea ice as a habitat for primary producers. In D. N. Thomas (Ed.), *Sea ice* (3rd ed., pp. 352–369). John Wiley & Sons, Ltd. https://doi.org/10.1002/9781118778371.ch14

Arrigo, K. R., Dieckmann, G., Gosselin, M., Robinson, D., Fritsen, C., & Sullivan, C. (1995). High resolution study of the platelet ice ecosystem in McMurdo Sound, Antarctica: Biomass, nutrient, and production profiles within a dense microalgal bloom. *Marine Ecology Progress Series*, *127*, 255–268. https://doi.org/10.3354/meps127255

Arrigo, K. R., Kremer, J. N., & Sullivan, C. W. (1993). A simulated Antarctic fast ice ecosystem. *Journal of Geophysical Research: Oceans*, *98*(C4), 6929–6946. https://doi.org/10.1029/93JC00141

Arrigo, K. R., Sullivan, C. W., & Kremer, J. N. (1991). A bio-optical model of Antarctic sea ice. *Journal of Geophysical Research*, *96*(C6), 10581. https://doi.org/10.1029/91JC00455

Arrigo, K. R., & Thomas, D. N. (2004). Large scale importance of sea ice biology in the Southern Ocean. *Antarctic Science*, *16*(4), 471–486. https://doi.org/10.1017/S0954102004002263

Arrigo, K. R., van Dijken, G. L., & Bushinsky, S. (2008). Primary production in the Southern Ocean, 1997-2006. *Journal of Geophysical Research: Oceans*, *113*(8), 1997–2006. https://doi.org/10.1029/2007JC004551

Arrigo, K. R., Worthen, D. L., Dixon, P. L., & Lizotte, M. P. (1998). Primary productivity of near surface communities within Antarctic pack ice. In P. Lizotte, & K. R. Arrigo (Eds.), *Antarctic Research Series* (Vol. 73, pp. 23–43). American Geophysical Union. https://doi.org/10.1029/AR073p0023

Arrigo, K. R., Worthen, D. L., Lizotte, M. P., Dixon, P., & Dieckmann, G. (1997). Primary production in Antarctic sea ice. *Science*, *276*(5311), 394–397. https://doi.org/10.1126/SCIENCE.276.5311.394

Behrendt, A., Dierking, W., & Witte, H. (2015). Thermodynamic sea ice growth in the central Weddell Sea, observed in upward-looking sonar data. *Journal of Geophysical Research: Oceans*, *120*(3), 2270–2286. https://doi.org/10.1002/2014JC010408

Bracegirdle, T. J., Krinner, G., Tonelli, M., Haumann, F. A., Naughten, K. A., Rackow, T., et al. (2020). Twenty first century changes in Antarctic and Southern Ocean surface climate in CMIP6. *Atmospheric Science Letters*, *21*(9). https://doi.org/10.1002/asl.984

Cheng, L., Von Schuckmann, K., Abraham, J. P., Trenberth, K. E., Mann, M. E., Zanna, L., et al. (2022). Past and future ocean warming. *Nature Reviews Earth & Environment*, *3*(11), 776–794. https://doi.org/10.1038/s43017-022-00345-1

Cimoli, E., Meiners, K. M., Lund-Hansen, L. C., & Lucieer, V. (2017). Spatial variability in sea-ice algal biomass: An under-ice remote sensing perspective. *Advances in Polar Science*, *28*(4), 29. https://doi.org/10.13679/j.advps.2017.4.00268

Comiso, J. C., Cavalieri, D., & Markus, T. (2003). Sea ice concentration, ice temperature, and snow depth using AMSR-E data. *IEEE Transactions on Geoscience and Remote Sensing*, *41*(2), 243–252. https://doi.org/10.1109/TGRS.2002.808317

Comiso, J. C., Kwok, R., Martin, S., & Gordon, A. L. (2011). Variability and trends in sea ice extent and ice production in the Ross Sea. *Journal of Geophysical Research*, *116*(C4), C04021. https://doi.org/10.1029/2010JC006391

Cota, G. F., & Sullivan, C. W. (1990). Photoadaptation, growth and production of bottom ice algae in the Antarctic. *Journal of Phycology*, *26*(3), 399–411. https://doi.org/10.1111/j.0022-3646.1990.00399.x

Deal, C., Jin, M., Elliott, S., Hunke, E., Maltrud, M., & Jeffery, N. (2011). Large-scale modeling of primary production and ice algal biomass within arctic sea ice in 1992. *Journal of Geophysical Research: Oceans*, *116*(7), 1–14. https://doi.org/10.1029/2010JC006409

Del Castillo, C. E., Signorini, S. R., Karaköylü, E. M., & Rivero-Calle, S. (2019). Is the Southern Ocean getting greener? *Geophysical Research Letters*, *46*(11), 6034–6040. https://doi.org/10.1029/2019GL083163

Dobson, F. W., & Smith, S. D. (1988). Bulk models of solar radiation at sea. *Quarterly Journal of the Royal Meteorological Society*, *114*(479), 165–182. https://doi.org/10.1002/qj.49711447909

Dupont, F. (2012). Impact of sea-ice biology on overall primary production in a biophysical model of the pan-Arctic Ocean. *Journal of Geophysical Research: Oceans*, *117*(8), 1–18. https://doi.org/10.1029/2011JC006983

Eayrs, C., Li, X., Raphael, M. N., & Holland, D. M. (2021). Rapid decline in Antarctic sea ice in recent years hints at future change. *Nature Geoscience*, *14*(7), 460–464. https://doi.org/10.1038/s41561-021-00768-3

Fetterer, F., Knowles, K., Meier, W. N., Savoie, M., & Windnagel, A. K. (2017). Sea Ice Index, Version 3 [Dataset]. NSIDC. https://doi.org/10.7265/N5K072F8

Fogt, R. L., & Marshall, G. J. (2020). The Southern Annular Mode: Variability, trends, and climate impacts across the Southern Hemisphere. *WIREs Climate Change*, *11*(4). https://doi.org/10.1002/wcc.652

Goutte, A., Charrassin, J., Cherel, Y., Carravieri, A., De Grissac, S., & Massé, G. (2014). Importance of ice algal production for top predators: New insights using sea-ice biomarkers. *Marine Ecology Progress Series*, *513*, 269–275. https://doi.org/10.3354/meps10971

Gregg, W. W., & Carder, K. L. (1990). A simple spectral solar irradiance model for cloudless maritime atmospheres. *Limnology & Oceanography*, *35*(8), 1657–1675. https://doi.org/10.4319/lo.1990.35.8.1657

Grömping, U. (2006). Relative importance for linear regression in R: The package relaimpo. *Journal of Statistical Software*, *17*(1), 1–27. https://doi.org/10.18637/jss.v017.i01

Grossi, S. M. G., Kottmeier, S. T., Moe, R. L., Taylor, G. T., & Sullivan, C. W. (1987). Sea ice microbial communities. VI. Growth and primary production in bottom ice under graded snow cover. *Marine Ecology Progress Series*, *35*, 153–164. https://doi.org/10.3354/meps035153

Grotti, M., Soggia, F., Ianni, C., & Frache, R. (2005). Trace metals distributions in coastal sea ice of Terra Nova Bay, Ross Sea, Antarctica. *Antarctic Science*, *17*(2), 289–300. https://doi.org/10.1017/S0954102005002695

Guglielmo, L., Carrada, G. C., Catalano, G., Dell'Anno, A., Fabiano, M., Lazzara, L., et al. (2000). Structural and functional properties of sympagic communities in the annual sea ice at Terra Nova Bay (Ross Sea, Antarctica). *Polar Biology*, *23*(2), 137–146. https://doi.org/10.1007/s003000050019

Heil, P., Allison, I., & Lytle, V. I. (1996). Seasonal and interannual variations of the oceanic heat flux under a landfast Antarctic sea ice cover. *Journal of Geophysical Research: Oceans*, *101*(C11), 25741–25752. https://doi.org/10.1029/96JC01921

Henson, S. A., Sarmiento, J. L., Dunne, J. P., Bopp, L., Lima, I., Doney, S. C., et al. (2010). Detection of anthropogenic climate change in satellite records of ocean chlorophyll and productivity. *Biogeosciences*, *7*(2), 621–640. https://doi.org/10.5194/bg-7-621-2010

Hobbs, W. R., Massom, R., Stammerjohn, S., Reid, P., Williams, G., & Meier, W. (2016). A review of recent changes in Southern Ocean sea ice, their drivers and forcings. *Global and Planetary Change*, *143*, 228–250. https://doi.org/10.1016/j.gloplacha.2016.06.008

Holland, P. R., Bruneau, N., Enright, C., Losch, M., Kurtz, N. T., & Kwok, R. (2014). Modeled trends in Antarctic sea ice thickness. *Journal of Climate*, *27*(10), 3784–3801. https://doi.org/10.1175/JCLI-D-13-00301.1

Holland, P. R., & Kwok, R. (2012). Wind-driven trends in Antarctic sea-ice drift. *Nature Geoscience*, *5*(12), 872–875. https://doi.org/10.1038/ngeo1627

Hosking, J. S., Orr, A., Bracegirdle, T. J., & Turner, J. (2016). Future circulation changes off West Antarctica: Sensitivity of the Amundsen Sea Low to projected anthropogenic forcing. *Geophysical Research Letters*, *43*(1), 367–376. https://doi.org/10.1002/2015GL067143

Hussain, M., & Mahmud, I. (2019). pyMannKendall: A python package for non parametric Mann Kendall family of trend tests. *Journal of Open Source Software*, *4*(39), 1556. https://doi.org/10.21105/joss.01556

Jin, M., Deal, C., Lee, S. H., Elliott, S., Hunke, E., Maltrud, M., & Jeffery, N. (2012). Investigation of Arctic sea ice and ocean primary production for the period 1992-2007 using a 3-D global ice-ocean ecosystem model. *Deep-Sea Research Part II Topical Studies in Oceanography*, *81–84*, 28–35. https://doi.org/10.1016/j.dsr2.2011.06.003

Kalnay, E., Kanamitsu, M., Kistler, R., Collins, W., Deaven, D., Gandin, L., et al. (1996). The NCEP/NCAR 40-year reanalysis project. *Bulletin of the American Meteorological Society*, *77*(3), 437–470. https://doi.org/10.1175/1520-0477(1996)077⟨0437:TNYRP⟩2.0.CO;2

Kendall, M. G. (1975). *Rank correlation methods*. Griffin.

Kohlbach, D., Graeve, M., Lange, B. A., David, C., Schaafsma, F. L., van Franeker, J. A., et al. (2018). Dependency of Antarctic zooplankton species on ice algae-produced carbon suggests a sea ice-driven pelagic ecosystem during winter. *Global Change Biology*, *24*(10), 4667–4681. https://doi.org/10.1111/gcb.14392

Kohlbach, D., Lange, B. A., Schaafsma, F. L., David, C., Vortkamp, M., Graeve, M., et al. (2017). Ice algae-produced carbon is critical for overwintering of Antarctic krill *Euphausia superba*. *Frontiers in Marine Science*, *4*, 310. https://doi.org/10.3389/fmars.2017.00310

Kusahara, K., Williams, G. D., Massom, R., Reid, P., & Hasumi, H. (2019). Spatiotemporal dependence of Antarctic sea ice variability to dynamic and thermodynamic forcing: A coupled ocean–sea ice model study. *Climate Dynamics*, *52*(7–8), 3791–3807. https://doi.org/10.1007/s00382-018-4348-3

Kwok, R. (2018). Arctic sea ice thickness, volume, and multiyear ice coverage: Losses and coupled variability (1958-2018). *Environmental Research Letters*, *13*(10), 105005. https://doi.org/10.1088/1748-9326/aae3ec

Langhorne, P. J., Hughes, K. G., Gough, A. J., Smith, I. J., Williams, M. J. M., Robinson, N. J., et al. (2015). Observed platelet ice distributions in Antarctic sea ice: An index for ocean-ice shelf heat flux. *Geophysical Research Letters*, *42*(13), 5442–5451. https://doi.org/10.1002/2015GL064508

Lazzara, L., Nardello, I., Ermanni, C., Mangoni, O., & Saggiomo, V. (2007). Light environment and seasonal dynamics of microalgae in the annual sea ice at Terra Nova Bay, Ross Sea, Antarctica. *Antarctic Science*, *19*(1), 83–92. https://doi.org/10.1017/S0954102007000119

Lei, R., Li, Z., Cheng, B., Zhang, Z., & Heil, P. (2010). Annual cycle of landfast sea ice in Prydz Bay, East Antarctica. *Journal of Geophysical Research*, *115*(C2), C02006. https://doi.org/10.1029/2008JC005223

Leppäranta, M. (1993). A review of analytical models of sea-ice growth. *Atmosphere-Ocean*, *31*(1), 123–138. https://doi.org/10.1080/07055900.1993.9649465

Lim, S. M., Payne, C. M., van Dijken, G. L., & Arrigo, K. R. (2022). Increases in Arctic sea ice algal habitat, 1985–2018. *Elementa: Science of the Anthropocene*, *10*(1), 00008. https://doi.org/10.1525/elementa.2022.00008

Lim, S. M., Van Dijken, G. L., & Arrigo, K. R. (2023). Data used in publication: Spatial and interannual variability of Antarctic sea ice bottom algal habitat, 2004–2019 [Dataset]. Stanford Digital Repository. https://doi.org/10.25740/JN797CV3253

Lindeman, R. H., Merenda, P. F., & Gold, R. Z. (1980). *Introduction to bivariate and multivariate analysis*. Scott, Foresman.

Mann, H. B. (1945). Nonparametric tests against trend. *Econometrica*, *13*(3), 245. https://doi.org/10.2307/1907187

Markus, T., & Cavalieri, D. J. (1998). Snow depth distribution over sea ice in the Southern Ocean from satellite passive microwave data. In M. O. Jeffries (Ed.), *Antarctic Research Series* (Vol. 74, pp. 19–39).

Marshall, G. J. (2007). Half-century seasonal relationships between the Southern Annular Mode and Antarctic temperatures. *International Journal of Climatology*, *27*(3), 373–383. https://doi.org/10.1002/joc.1407

Matear, R. J., O'Kane, T. J., Risbey, J. S., & Chamberlain, M. (2015). Sources of heterogeneous variability and trends in Antarctic sea-ice. *Nature Communications*, *6*(1), 8656. https://doi.org/10.1038/ncomms9656

McPhee, M. G. (1992). Turbulent heat flux in the upper ocean under sea ice. *Journal of Geophysical Research*, *97*(C4), 5365. https://doi.org/10.1029/92JC00239

McPhee, M. G., Ackley, S. F., Guest, P., Stanton, T. P., Huber, B. A., Martinson, D. G., et al. (1996). The Antarctic zone flux experiment. *Bulletin of the American Meteorological Society*, *77*(6), 1221–1232. https://doi.org/10.1175/1520-0477(1996)077⟨1221:TAZFE⟩2.0.CO;2

McPhee, M. G., Kottmeier, C., & Morison, J. H. (1999). Ocean heat flux in the central Weddell Sea during winter. *Journal of Physical Oceanography*, *29*(6), 1166–1179. https://doi.org/10.1175/1520-0485(1999)029⟨1166:OHFITC⟩2.0.CO;2

Meier, W., Fetterer, F., Windnagel, A., & Stewart, S. (2021). NOAA/NSIDC Climate Data Record of Passive Microwave Sea Ice Concentration, Version 4 [Dataset]. NASA National Snow and Ice Data Center Distributed Active Archive Center. https://doi.org/10.7265/EFMZ-2T65

Meiners, K. M., Vancoppenolle, M., Thanassekos, S., Dieckmann, G. S., Thomas, D. N., Tison, J. L., et al. (2012). Chlorophyll *a* in Antarctic sea ice from historical ice core data. *Geophysical Research Letters*, *39*(21), 1–6. https://doi.org/10.1029/2012GL053478

Mo, K. C. (2000). Relationships between low-frequency variability in the Southern Hemisphere and sea surface temperature anomalies. *Journal of Climate*, *13*(20), 3599–3610. https://doi.org/10.1175/1520-0442(2000)013⟨3599:RBLFVI⟩2.0.CO;2

Notz, D. (2012). Challenges in simulating sea ice in Earth System Models. *WIREs Climate Change*, *3*(6), 509–526. https://doi.org/10.1002/wcc.189

Parkinson, C. L. (2019). A 40-y record reveals gradual Antarctic sea ice increases followed by decreases at rates far exceeding the rates seen in the Arctic. *Proceedings of the National Academy of Sciences*, *116*(29), 14414–14423. https://doi.org/10.1073/pnas.1906556116

Perovich, D. K. (2002). Seasonal evolution of the albedo of multiyear Arctic sea ice. *Journal of Geophysical Research*, *107*(C10), 8044. https://doi.org/10.1029/2000JC000438

Perovich, D. K., Maykut, G. A., & Grenfell, T. C. (1986). Optical properties of ice and snow in the polar oceans. I: Observations. In M. A. Blizard (Ed.), *1986 Technical Symposium Southeast* (p. 232). https://doi.org/10.1117/12.964238

Petrich, C., & Eicken, H. (2017). Overview of sea ice growth and properties. In D. N. Thomas (Ed.), *Sea ice* (pp. 1–41). John Wiley & Sons, Ltd. https://doi.org/10.1002/9781118778371.ch1

Pinkerton, M. H., & Hayward, A. (2021). Estimating variability and long-term change in sea ice primary productivity using a satellite-based light penetration index. *Journal of Marine Systems*, *221*, 103576. https://doi.org/10.1016/j.jmarsys.2021.103576

Pringle, D. J., Eicken, H., Trodahl, H. J., & Backstrom, L. G. E. (2007). Thermal conductivity of landfast Antarctic and Arctic sea ice. *Journal of Geophysical Research*, *112*(C4), C04017. https://doi.org/10.1029/2006JC003641

Raphael, M. N., & Handcock, M. S. (2022). A new record minimum for Antarctic sea ice. *Nature Reviews Earth & Environment*, *3*(4), 215–216. https://doi.org/10.1038/s43017-022-00281-0

Saenz, B. T., & Arrigo, K. R. (2014). Annual primary production in Antarctic sea ice during 2005-2006 from a sea ice state estimate. *Journal of Geophysical Research: Oceans*, *119*(6), 3645–3678. https://doi.org/10.1002/2013JC009677

Saji, N., & Yamagata, T. (2003). Possible impacts of Indian Ocean Dipole mode events on global climate. *Climate Research*, *25*, 151–169. https://doi.org/10.3354/cr025151

Sen, P. K. (1968). Estimates of the regression coefficient based on Kendall's Tau. *Journal of the American Statistical Association*, *63*(324), 1379–1389. https://doi.org/10.1080/01621459.1968.10480934

Shen, X., & Ke, C.-Q. (2021). Snow depth product over Antarctic sea ice from 2002 to 2020 [Dataset]. National Tibetan Plateau Data Center. https://doi.org/10.11888/Snow.tpdc.271653

Shen, X., Ke, C.-Q., & Li, H. (2022). Snow depth product over Antarctic sea ice from 2002 to 2020 using multisource passive microwave radiometers. *Earth System Science Data*, *14*(2), 619–636. https://doi.org/10.5194/essd-14-619-2022

Shu, Q., Song, Z., & Qiao, F. (2015). Assessment of sea ice simulations in the CMIP5 models. *The Cryosphere*, *9*(1), 399–409. https://doi.org/10.5194/tc-9-399-2015

Trenerry, L., McMinn, A., & Ryan, K. (2002). In situ oxygen microelectrode measurements of bottom-ice algal production in McMurdo Sound, Antarctica. *Polar Biology*, *25*(1), 72–80. https://doi.org/10.1007/s003000100314

Tschudi, M., Meier, W. N., Stewart, J. S., Fowler, C., & Maslanik, J. (2019). Polar Pathfinder Daily 25 km EASE-Grid Sea Ice Motion Vectors, Version 4 [Dataset]. NASA National Snow and Ice Data Center Distributed Active Archive Center. https://doi.org/10.5067/INAWUWO7QH7B

van Leeuwe, M. A., Tedesco, L., Arrigo, K. R., Assmy, P., Campbell, K., Meiners, K. M., et al. (2018). Microalgal community structure and primary production in Arctic and Antarctic sea ice: A synthesis. *Elementa: Science of the Anthropocene*, *6*(1). https://doi.org/10.1525/elementa.267

Virtanen, P., Gommers, R., Oliphant, T. E., Haberland, M., Reddy, T., Cournapeau, D., et al. (2020). SciPy 1.0: Fundamental algorithms for scientific computing in Python. *Nature Methods*, *17*(3), 261–272. https://doi.org/10.1038/s41592-019-0686-2

Wadhams, P., Lange, M. A., & Ackley, S. F. (1987). The ice thickness distribution across the Atlantic sector of the Antarctic Ocean in midwinter. *Journal of Geophysical Research*, *92*(C13), 14535. https://doi.org/10.1029/JC092iC13p14535

Wang, J., Luo, H., Yang, Q., Liu, J., Yu, L., Shi, Q., & Han, B. (2022). An unprecedented record low Antarctic sea-ice extent during austral summer 2022. *Advances in Atmospheric Sciences*, *39*(10), 1591–1597. https://doi.org/10.1007/s00376-022-2087-1

Webster, M., Gerland, S., Holland, M., Hunke, E., Kwok, R., Lecomte, O., et al. (2018). Snow in the changing sea-ice systems. *Nature Climate Change*, *8*(11), 946–953. https://doi.org/10.1038/s41558-018-0286-7

Wilson, E. A., Riser, S. C., Campbell, E. C., & Wong, A. P. S. (2019). Winter upper-ocean stability and ice–ocean feedbacks in the sea ice–covered Southern Ocean. *Journal of Physical Oceanography*, *49*(4), 1099–1117. https://doi.org/10.1175/JPO-D-18-0184.1

Worby, A. P., Geiger, C. A., Paget, M. J., Van Woert, M. L., Ackley, S. F., & De Liberty, T. L. (2008). Thickness distribution of Antarctic sea ice. *Journal of Geophysical Research*, *113*(C5), C05S92. https://doi.org/10.1029/2007JC004254

Yue, S., & Wang, C. (2004). The Mann-Kendall Test modified by effective sample size to detect trend in serially correlated hydrological series. *Water Resources Management*, *18*(3), 201–218. https://doi.org/10.1023/B:WARM.0000043140.61082.60

References From the Supporting Information

Fox, J., & Weisberg, S. (2019). *An R compainion to applied regression* (3rd ed.). Sage.

James, G., Witten, D., Hastie, T., & Tibshirani, R. (2013). *An introduction to statistical learning* (Vol. 103). Springer New York. https://doi.org/10.1007/978-1-4614-7138-7

White, H. (1980). A heteroskedasticity-consistent covariance matrix estimator and a direct test for heteroskedasticity. *Econometrica*, *48*(4), 817. https://doi.org/10.2307/1912934

Zeileis, A., & Hothorn, T. (2002). Diagnostic checking in regression relationships. *R News*, *2*(3), 7–10.